

# A Novel MRI Method for Breast Cancer Detection Based on Diffusion Tensor Tracking of the Ductal Trees

E. Eyal<sup>1</sup>, M. Shapiro-Feinberg<sup>2</sup>, E. Furman Haran<sup>1</sup>, D. Grobgeld<sup>1</sup>, T. Golan<sup>3</sup>, Y. Itzhak<sup>3</sup>, R. Catane<sup>3</sup>, M. Papa<sup>3</sup>, and H. Degani<sup>1</sup>

<sup>1</sup>Weizmann Institute of Science, Rehovot, Israel, <sup>2</sup>Meir Medical Center, Kfar Saba, Israel, <sup>3</sup>Sheba Medical Center, Tel Hashomer, Israel

## Purpose:

Our goal is to characterize the anisotropic water diffusion properties in the mammary ductal trees tissue using diffusion tensor MRI and to utilize this method to detect breast cancer without the injection of a contrast-agent.

## Introduction:

Early detection of breast cancer by x-ray mammography and ultrasound has insufficient sensitivity and specificity particularly for detecting lesions in dense breasts. Dynamic contrast enhanced (DCE) MRI is used for detection and diagnosis of breast cancer only for special cases, presumably because of its relatively high costs, significant false positive rates, discomfort and risk of adverse effects, including nephrogenic systemic fibrosis. Recently, it was shown that apparent diffusion coefficient (ADC) values can help distinguish between cancers, benign lesions and normal breast tissue. However, ADC maps are not sufficiently sensitive for establishing a stand alone method for breast cancer detection. Our knowledge of the ductal system is based on several detailed anatomical studies of breast autopsies and mastectomy specimens (1) but none of the available imaging methods employed today has succeeded in tracking the full ductal tree. We propose that mapping the anisotropic water diffusion properties of the ducts can help meet this challenge (2). Furthermore, since mammary malignancies typically develop from the ductal epithelial cells, and spread within the ducts (ductal carcinoma in situ-DCIS) before penetrating the ducts' walls (infiltrating ductal /lobular carcinoma-IDC/ILC), changes in the ductal diffusion tensor may serve as a biomarker/bio-imaging enabling earlier detection of malignant cell behavior.

## Methods:

**Subjects:** This study included 21 healthy female volunteers with no current indications of breast pathological findings in mammography and ultrasound and 13 patients with 15 biopsy confirmed breast cancers (IDC, ILC and DCIS). All protocols were approved by the Internal Review Board of Meir Medical Center (Kfar Sabah, Israel) and a signed informed consent was obtained from all subjects.

**Magnetic Resonance Imaging scans:** Images were acquired on a 3 Tesla whole body MRI scanner: MAGNETOM Trio, Tim System (Siemens) equipped with a transmitting body coil and a receiving, 4 channels breast array coil (Siemens) or 7 channel breast array coil (Invivo). The MRI protocol included transversal T2 weighted images with and without fat saturation, axial DTI with Fat-Saturation, and a DCE-MRI protocol that was applied only to patients with confirmed cancers. The field of view included the two breast ranging from 360 to 390 mm, and 60 slices were acquired with slice thickness of 2-2.5 mm, covering the whole breasts. The DTI data sets were acquired using the twice refocused echo planar imaging sequence (3). 2D DTI datasets were acquired using diffusion sensitizing gradient in 64 directions at two b values, 0 and 700 mm<sup>2</sup>s<sup>-1</sup>; echo-time/repetition time of 120ms/10400 ms and spatial resolution of 1.9x1.9x2mm<sup>3</sup>, or 1.9x1.9x2.5mm<sup>3</sup>.

**Data processing:** The diffusion weighted images were analyzed using a MATLAB programming environment (v7.0.1, MathWorks, Inc., Natick, MA). The diffusion tensor was calculated, pixel by pixel, by non linear fitting of the diffusion dataset to Stejskal-Tanner equation (4) using the general tensor form of the diffusion coefficient D. The tensor was diagonalized by principal component analysis (PCA) yielding 3 eigenvectors and their corresponding eigen-values  $\lambda_1$ ,  $\lambda_2$  and  $\lambda_3$ . The eigen-values were presented in color coded maps. The anisotropy was expressed by an anisotropy factor defined as the subtraction  $\lambda_1 - \lambda_3$ . We also calculated the values per pixel of the average apparent diffusion coefficient (ADC) defined as the average of the three eigen-values. The diffusion parameters were color coded and overlaid on the corresponding T2 weighted images. For the breast cancer patients, the dynamic contrast enhanced dataset was obtained and analyzed using the 3TP method (5-6).

**Statistical Analysis:** Percentile values of the three diffusion parameters  $\lambda_1$ ,  $\lambda_2$  and  $\lambda_3$  were calculated for the entire fibro-glandular tissue of the breasts in the healthy volunteers and within the ROI of the cancers delineated manually based on correlation with the enhancement in DCE-MRI images and the histopathological findings. Unpaired, two tailed t-test was applied for evaluating statistical differences between the diffusion parameters for the fibro-glandular tissue in healthy volunteers and cancerous lesions.

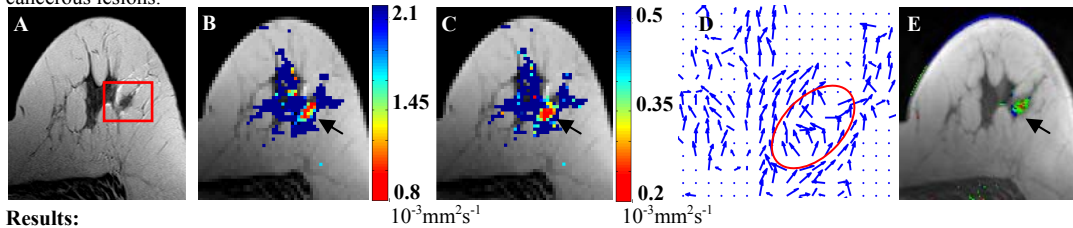


**Fig 1:** Diffusion tensor analysis. (A) T2w of the right breast. (B) Parametric map of the diffusion coefficient  $\lambda_1$  and (C) the anisotropy factor  $\lambda_1 - \lambda_3$ . (D) Vector map for the first eigenvector,  $v_1$  in the region delineated in (A), with the lesion location is marked by a red ellipse. (E) Contrast enhanced MRI color coded by the 3TP method (5-6).

## Results:

Statistical evaluation for the values of  $\lambda_1$ ,  $\lambda_2$ ,  $\lambda_3$  in the fibro-glandular tissue of healthy volunteers compared to cancerous regions in the patients has indicated that there is a significant difference between the groups for all three diffusion indexes. The largest eigen-value in healthy fibro-glandular tissue,  $\lambda_1$ , was  $(2.1 \pm 0.2) \times 10^{-3} \text{mm}^2 \text{s}^{-1}$ , and showed the most significant difference vs. cancerous tissue ( $p < 0.0001$ ) with mean difference between the groups of  $(1.2 \pm 0.2) \times 10^{-3} \text{mm}^2 \text{s}^{-1}$ . In addition, for healthy tissue, the mean for the anisotropic factor,  $\lambda_1 - \lambda_3$ , was  $(0.8 \pm 0.1) \times 10^{-3} \text{mm}^2 \text{s}^{-1}$  and also significantly different between cancer and normal tissue ( $p < 0.0001$ ) with mean difference of  $(0.5 \pm 0.1) \times 10^{-3} \text{mm}^2 \text{s}^{-1}$ . The  $\lambda_1$  and  $\lambda_1 - \lambda_3$  parametric maps clearly demonstrate that the cancer lesion, pointed by the black arrow, has significantly lower values compare to the surrounding normal tissue (Fig 1 B&C). In addition the vector map of the first eigenvector (Fig 1 D), delineated by the red box in A, showed that there is a lack of directionality inside the lesion area (red ellipse) compared to the surrounding tissue. The location of the lesion was confirmed by the contrast enhanced MRI as presented in Fig 1 E with the cancer lesion pointed by the black arrow.

## Conclusions:

We have shown that DTI based MRI reveals the diffusion anisotropy in the mammary ducts and the changes in the diffusion tensor components due to cancer growth. We found three critical diffusion parameters that simultaneously change in breast cancers: reduction in the value of the diffusion coefficient  $\lambda_1$ , reduction in the anisotropy factor  $\lambda_1 - \lambda_3$  and random orientation in the direction of the diffusion vector  $v_1$  inside the lesion. Overall this method uses intrinsic contrast based on water anisotropic diffusion, and hence is exclusively non invasive and non hazardous. It is performed within a reasonable time frame of 10 min and could be shortened by decreasing the number of the diffusion gradient from 64 to 30. Further studies to characterize the diffusion properties of benign breast diseases and assess the DTI specificity for distinguishing cancer from benign lesions are now underway.

**References:** 1. Going, J. J. Breast Cancer Res, 8: 107, 2006. 2. Eyal E. *et al*, prog 508, ISMRM, 2008. 3. Reese, TG *et al*. MRM, 49:177-182, 2003. 4. Stejskal, E. O. and Tanner, J. E. JCP. Vol 42(1):288-292, 1965. 5. Degani *et al* Nature Medicine 3(7):780-782, 1997. 6. Kelcz F *et al*. Am J Roentgenol 179(6):1485-1492, 2002.

Supported by Israel Science Foundation 235/08